Trapping light in a ring resonator using a grating-assisted coupler with asymmetric transmission

Mykola Kulishov [a, b], Jacques M. Laniel [a], Nicolas Bélanger [a], David V. Plant [a]

[a] *Department of Electrical and Computer Engineering, Photonic System Group, McGill University, Montreal (Quebec) H3A 2A7, Canada*
jlaniel@ photonics.ece.mcgill.ca , nbelan@ photonics.ece.mcgill.ca , plant@photonics.ece.mcgill.ca
[b] *Adtek Photomask Inc., 4950 Fisher str., Montreal (Quebec) H4T 1J6, Canada*
mkulishov@adetkphotomask.com

Abstract: A recently proposed concept suggests that a matched periodic modulation of both the refractive index and the gain/loss of the media breaks the coupling symmetry of the two co-propagating modes and allows only a unidirectional coupling from the *i*-th mode to *j*-the mode but not the opposite. This concept has been used to design a ring resonator coupled through a complex grating composed of both real (index) and imaginary (loss/gain) parts according to Euler relation: $\Delta n = n_0 \exp(-jkx) = n_0 (\cos(kx) - j \sin(kx))$. Such asymmetrical coupling allows light to be coupled into the ring without letting it out. We present a detailed theoretical analysis of the ring resonator in the linear regime, and we investigate its linear temporal dynamics. Three possible states of the complex grating leads to the possibility of developing a dynamic optical memory cell where, for example, a data modulated train of optical pulses can be stored. This data can be accessed without destroying it, and can also be erased thus permitting the storage of a new bit. Finally, the ring can be used for pulse retiming.

OCIS codes: (230.3120) Integrated optics devices; (200.4740) Optical processing, (210.4680) Optical memories

References and links

1. A. Rebane, J. Feinberg, "Time-resolved holography," Letters to Nature **351**, 378-380 (1991).
2. A. Armitage, S. Skolnik, A.V. Kavokin, D.M. Whittaker, V.N. Astratov, G.A. Gehring, J.S. Roberts, "Polariton-induced optical asymmetry in semiconductor microcavities," Phys. Rev. B **58,** 15367-15370 (1998).
3. G.S. Agarwal, S.D. Gupta, "Reciprocity relations for reflected amplitudes," Opt. Lett. **27,** 1205-1207 (2002).
4. R.J. Potton, "Reciprocity in optics," Rep. Prog. Phys. **67,** 717-754 (2004).
5. V.S.C. M. Rao, S. D. Gupta, G.S. Agarwal, "Study of asymmetric multilayered structures by means of nonreciprocity in phases," J. Opt. B: Quantum Semiclass. Opt. **6,** 555-562 (2004).
6. L. Poladian, "Resonance mode expansions and exact solutions for nonuniform gratings," Phys. Rev. E **54**, 2963-2975 (1996).
7. M. Kulishov, J.M. Laniel, N. Bélanger, J. Azana, D.V. Plant, "Nonreciprocal waveguide Bragg gratings," Opt. Express **13**, 3068-3078 (2005), http://www.opticsexpress.org/abstract.cfm?URI=OPEX-13-8-3068.
8. M. Greenberg, M. Orenstein, "Irreversible coupling by use of dissipative optics," Opt. Lett. **29**, 451-453 (2004).
9. M. Greenberg, M. Orenstein, "Unidirectional complex gratings assisted couplers," Opt. Express **12**, 4013-4018 (2004), http://www.opticsexpress.org/abstract.cfm?URI=OPEX-12-17-4013.
10. M. Greenberg, "Unidirectional mode devices based on irreversible mode coupling," MSc. Thesis, Israel Institute of Technology, Haifa, March, 2004.
11. R.R.A. Syms, S. Makrimichalou, A.S. Holms, "High-speed optical signal processing potential of grating-coupled waveguide filters," Appl. Opt. **30**, 3762-3769 (1991).

#6760 - $15.00 US Received 4 March 2005; revised 27 April 2005; accepted 27 April 2005

1. Introduction

Nonreciprocal behavior in optical diffraction has been demonstrated experimentally [1, 2] and studied theoretically [3, 4, 5]. Using identical modulations for both the refractive index and the loss/gain, unidirectional mode coupling has been proposed and studied within reflective gratings [6,7], as well as between co-propagating modes of a co-directional coupler [8, 9]. Within the asymmetrical grating-assisted co-directional coupler (A-GACC), the asymmetric mode interaction depends on the phase relation between the real and imaginary parts of the complex grating along the propagation direction, e.g. $\pi/2$ or $-\pi/2$. As a result, a signal injected into one input port of the A-GACC will be transferred to both outputs while a signal injected into the other input port will remain in the same waveguide.

This asymmetrical behavior creates the possibility to design and build new devices with interesting functionalities. One of these devices offering many interesting features is an A-GACC where one of the waveguide outputs is connected to its corresponding input, thus creating a ring resonator. This structure has been proposed by Greenberg in Ref. [10], but to date has not been studied. The present paper introduces a mathematical description of an A-GACC based on the coupled mode theory, and offers the analytical framework to investigate rigorously the different functionalities provided by the A-GACC with a ring resonator. The asymmetric behavior of the A-GACC provides the possibility of capturing a signal inside the ring. It would therefore act exactly as an optical memory. Furthermore, if the complex grating is switchable, it is also possible to extract the signal from the ring. The extraction can be done in two ways: i) by retrieving a copy of the signal and preserving it inside the ring or ii) by removing (or clearing) the signal from the ring. Retrieving can be achieved by changing the phase relation of the complex grating, while removing the signal (ring clearing) can be performed only by reducing the A-GACC to a symmetrical GACC. All of these possible configurations offer rich temporal dynamics creating the possibility of a wide variety of applications. In this paper we study two cases: the memory cell and the pulse retimer.

The paper is organized as follows. Section 2 presents the structure and the spectral characteristics of the A-GACC with the ring resonator. Section 3 describes the mechanism that allows the trapping of a signal inside the ring, as well as the mechanisms that allow duplication or extraction of this trapped signal. Section 4 presents the temporal dynamics of the ring resonator, and Section 5 discusses the possible applications of such devices. Finally Section 6 concludes the paper.

2. Spectral characteristics of switchable Asymmetric GACC

The waveguide structure of the A-GACC is shown in Fig. 1(a). It consists of two asynchronous parallel waveguides (i.e. the propagation constants of the two waveguides are not equal) in a close proximity to one another. The lower and upper waveguide are labeled guide #1 and #2, respectively and their propagation constants are β_1 and β_2. It will be assumed that $\beta_1 > \beta_2$. For simplicity and clarity, we limit the analysis to the situation where the two guides of the GACC are far from synchronism and weakly coupled, i.e. the only mode interaction mechanism is the one induced by the grating perturbation.

Spectral characteristics of the asymmetric interaction in the A-GACC have been studied based on coupled-mode equations formalism. The complex grating in the A-GACC is described by the following expression:

$$\Delta n = \Delta n_{DC} + j\frac{\Delta\alpha_{DC}}{k_0} + \Delta n_{AC}\cos\left(\frac{2\pi}{\Lambda}z\right) - j\frac{\Delta\alpha_{AC}}{k_0}\sin\left(\frac{2\pi}{\Lambda}z\right), \quad (1)$$

where Λ is the grating period, Δn_{DC} and Δn_{AC} are respectively the constant and modulated perturbation to the refractive index, $\Delta\alpha_{DC}$ and $\Delta\alpha_{AC}$ are respectively the constant and modulated perturbation to the field amplitude gain/loss and $k_0 = 2\pi/\lambda$ where λ is the wavelength in vacuum.

#6760 - $15.00 US Received 4 March 2005; revised 27 April 2005; accepted 27 April 2005

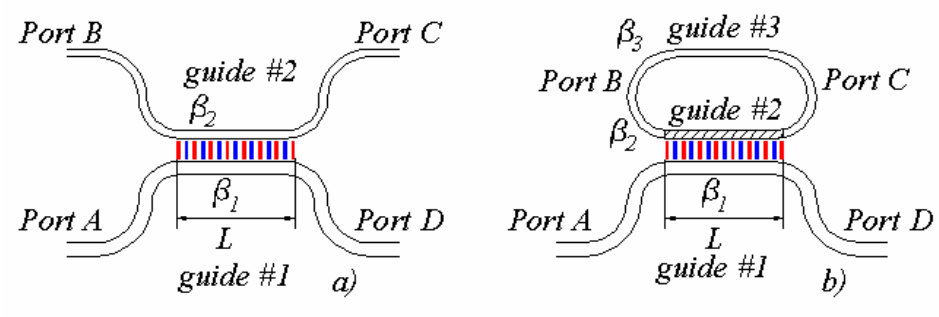

Fig. 1. (a) Grating assisted co-directional coupler (GACC) and (b) a ring resonator coupled with the guide by the complex grating. The propagation constants of the guides are given by β_1 and β_2, the guides are asynchronous ($\beta_1 > \beta_2$). The grating length is given by L.

The solution of the coupled mode equations for the perturbation given by Eq. (1) can be expressed by using a matrix formalism linking the signal at Ports A and B (as shown in Fig. 1(a)) corresponding to $z = 0$ and the signal at Ports C and D corresponding to $z = L$.

$$\begin{bmatrix} \overline{E}_D \\ \overline{E}_C \end{bmatrix} = \mathbf{M} \begin{bmatrix} \overline{E}_A \\ \overline{E}_B \end{bmatrix} = \begin{bmatrix} M_{11} & M_{12} \\ M_{21} & M_{22} \end{bmatrix} \begin{bmatrix} \overline{E}_A \\ \overline{E}_B \end{bmatrix}, \tag{2}$$

where the M_{ij} are the elements of the transmission matrix **M** and the bar over the electric fields E_j indicates that they are represented in the Fourier domain. The transfer matrix Eq. (3) is obtained through a similar process as the one used in Ref. [5]:

$$\mathbf{M} = T_{avg}\psi_{avg} \begin{bmatrix} \tilde{a}_+ \psi_{+g} & j(\kappa_n - \kappa_\alpha) L \operatorname{sinc}(\tilde{\gamma}L)\psi_{+g} \\ j(\kappa_n + \kappa_\alpha) L \operatorname{sinc}(\tilde{\gamma}L)\psi_{-g} & \tilde{a}_- \psi_{-g} \end{bmatrix} \tag{3}$$

where $\tilde{\gamma} = \left[\left(\Delta\tilde{\beta}\right)^2 + \kappa_n^2 - \kappa_\alpha^2 \right]^{1/2}$, $\tilde{a}_\pm = \cos(\tilde{\gamma}L) \pm j\Delta\tilde{\beta} L \operatorname{sinc}(\tilde{\gamma}L)$ and $\psi_{\pm g} = \exp(\pm j\pi L/\Lambda)$. T_{avg} and ψ_{avg} represent the amplitude and phase transmission coefficients of the A-GACC averaged on its two guides, i.e. $T_{avg} = (T_1 T_2)^{1/2}$ and $\psi_{avg} = (\psi_1 \psi_2)^{1/2}$. Throughout this paper, T_i and ψ_i are amplitude transfer coefficients for a waveguide (or subcase) labeled by the index "*i*". T_i refers to the magnitude of the transmission in amplitude:

$$T_i = \exp[-\alpha_i L], \tag{4}$$

while the ψ_i refers to a phase factor:

$$\psi_i = \exp[j\beta_i' L]. \tag{5}$$

The tilde on some other parameters indicates those, which could be complex. The off diagonal terms of Eq. (3) include combinations of κ_n and κ_α which are respectively proportional to the overlap between the real and imaginary AC parts of Eq. (1) and the spatial distribution of the propagating modes of the both guides. The complex phasematch condition is defined by $\Delta\tilde{\beta} = (\tilde{\beta}_1 - \tilde{\beta}_2)/2 - \pi/\Lambda$, where the complex propagation constants are $\tilde{\beta}_i = \beta_i + \sigma_i + j\alpha_i = \beta_i' + j\alpha_i$ (i = 1, 2). The coefficients σ_i and α_i are proportional to the overlap between the spatial mode distributions and the DC components of Eq. (1), respectively Δn_{DC} and $\Delta\alpha_{DC}/k_0$. The effect of gain or loss can be modeled by either taking $\alpha_i > 0$ for loss or $\alpha_i < 0$ for gain. The prime added to β_i' indicates that it is the perturbed

#6760 - $15.00 US
Received 4 March 2005; revised 27 April 2005; accepted 27 April 2005

propagation constant including the DC contribution of the grating to the refractive index. Things become more complicated with α_i because it transforms the propagation constant $\tilde{\beta}_i$ from a real to a complex quantity. On the other hand, $\tilde{\gamma}^2$ is still a real quantity if the DC gain/loss experienced by each guide is the same, e.g., $\alpha_1 = \alpha_2$. This parameter $\tilde{\gamma}$ is then real except near the phase match condition ($\Delta\tilde{\beta} = 0$) where it could be purely imaginary when the gain/loss grating is stronger than the index grating ($|\kappa_\alpha| > \kappa_n$).

The loss parameters and the coupling coefficients may be dispersive, but the response of this device as a function of wavelength (or frequency) is mainly driven by the propagation constants. If we neglect the dispersion, here is how the propagation constants are defined around the angular frequency $\omega_0 = k_0 c$ of the light injected into the device:

$$\beta_i'(\omega) = n_{eff,i}\frac{\omega_0}{c} + n_{g,i}\frac{\omega - \omega_0}{c}. \tag{6}$$

The indices $n_{eff,i}$ and $n_{g,i}$ are the effective and group indices of each guide, respectively. Using Eq. (6), it is now possible to evaluate the frequency dependence of the previously determined parameters. For instance, the phase transmission coefficient of each guide (Eq. (5)) could be written as follows:

$$\begin{aligned} \psi_i &= \psi_{i,0}\exp\left[j(\omega-\omega_0)\tau_i\right], \\ \psi_{i,0} &= \exp\left[j\, n_{eff,i}\omega_0 L/c\right], \\ \tau_i &= n_{g,i}L/2c, \end{aligned} \tag{7}$$

where $\psi_{i,0}$ is simply a constant phase factor. However τ_i is a meaningful parameter representing the group delay across the guide #"*i*". A typical time τ could also be associated with the phase match condition:

$$\begin{aligned} &\mathrm{Re}\left\{\Delta\tilde{\beta}\right\}L = \theta + (\omega-\omega_0)\tau, \\ &\theta = \left[\left(n_{eff,1} - n_{eff,2}\right)\frac{\omega_0}{2c} - \frac{\pi}{\Lambda}\right]L, \\ &\tau = \frac{n_{g,1} - n_{g,2}}{2c}L. \end{aligned} \tag{8}$$

The shorter τ is, the broader the bandwidth of the A-GACC will be. The A-GACC described at Eq. (3) becomes ideal if the magnitude of the imaginary part of the modulation is equal to the real part, i.e. when $\kappa_n = \kappa$ and $\kappa_\alpha = S\kappa$ with S equaling +1 or -1. One interesting feature that can extend the functionality of the A-GACC is the possibility of switching the phase relation between the real and imaginary grating. It requires controlling the sign S of the AC gain/loss grating in Eq. (1) ($S = \mathrm{sgn}(\Delta\alpha_{AC})$). Such control provides two distinct states: S = ±1. A third state would be the one where the imaginary grating is switched off, or S = 0. This particular state is still described by the general transfer matrix (Eq. (3)) where only $\tilde{\gamma}$ is modified by setting $\kappa_\alpha = 0$. For such a case, the A-GACC becomes a standard GACC.

Based on the above, we define $\mathbf{M}_S$ as the transfer matrix for S = ±1:

$$\mathbf{M}_S = \begin{bmatrix} T_1\psi_1 & 0 \\ 0 & T_2\psi_2 \end{bmatrix} + j\kappa L\,\mathrm{sinc}\left(\Delta\tilde{\beta}L\right)T_{avg}\psi_{avg}\begin{bmatrix} 0 & (1-S)\psi_{+g} \\ (1+S)\psi_{-g} & 0 \end{bmatrix} \tag{9}$$

The asymmetrical behavior of the A-GACC becomes obvious through Eq. (9) since one of the off-diagonal elements is zero if S = +1 or –1. The case of S = +1 implies that $\kappa_n = \kappa_\alpha$ which means that both Δn_{AC} and $\Delta\alpha_{AC}$ in Eq. (1) have the same sign, namely positive. In one period of this grating along the propagation direction, a local maximum of the index of

#6760 - $15.00 US Received 4 March 2005; revised 27 April 2005; accepted 27 April 2005

refraction is followed by a maximum of gain, a minimum of index of refraction, and finally a maximum of loss. According to Eq. (9), this A-GACC couples the light injected into Port A to both output Ports C and D, but it prevents any light injected into Port B from being coupled into Port D. This device is said to be asymmetrical because its coupling behavior between the two guides is reversed when the light is launched into Ports C and D. In such a case, the light injected into those Ports sees a grating with a maximum of loss just after a maximum of index of refraction, which corresponds to the state S = -1. Therefore, the symmetry of the coupler is now reversed. It is now the light launched into guide #1 through Port D that can not couple at all in its cross state while the other input does (Port C).

In order to illustrate the spectral characteristics of an ideal A-GACC, the transmission is plotted in Fig 2 for the case where a signal is injected in Port A. The effective indices of the guides are $n_{eff,1}$ = 1.519375 and $n_{eff,2}$ =1.500000. For the sake of simplicity, we assume that the effective indices are frequency independent, so they are equal to their respective group indices ($n_{g,i} = n_{eff,i}$). The grating length is L = 25 mm and its period is Λ = 80 μm which satisfies the phase-matching condition at the central wavelength of 1.55 μm. The grating strength is $\kappa L = \pi/2$ or $(\kappa_n + \kappa_\alpha)L = \pi$, where $\kappa_n + \kappa_\alpha$ is the coupling coefficient from guide #1 to guide #2. This grating strength is chosen so that if the imaginary part of the grating is removed, the resulting symmetrical GACC provides complete signal coupling from one guide to the other at the resonance wavelength.

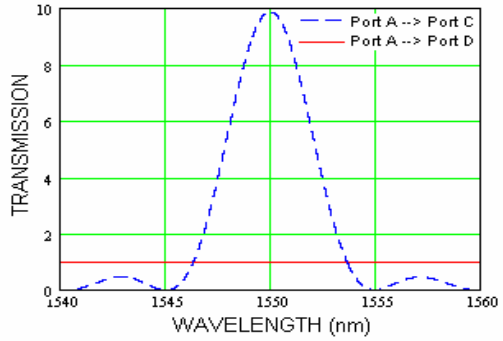

Fig. 2. Transmission spectra of an A-GACC for bar-state (solid, red) and cross-state (dash, blue) for $\kappa L = \pi/2$, L = 25 mm, Λ = 80 μm. The signal is launched into Port A

The signal launched into Port A of the A-GACC passes into Port D without any changes (solid, red). At the same time there is strong coupling of the launched signal into Port C at the resonance wavelength (dash, blue). It is important to point out that in our calculations we neglect any contributions from the DC gain/loss component of Eq. (1), which means that $\alpha_1 = \alpha_2 = 0$.

It is worth noting that the imaginary grating of Eq. (1) consists of equal segments of gain and loss, which implies that there is no net gain or loss during the propagation. Despite this zero average gain, there is an amplification of the coupled signal around the resonance wavelength. The explanation of this effect [8, 9] is that two co-propagating modes interact constructively in the gain region of the imaginary grating. For light coupled into Port B, complex, single-sideband perturbation prevents coupling into Port D, and signal passes from Port B into Port C without any changes (flat spectral characteristic) as predicted by Eq. (9).

3. Spectral characteristic and operation of an A-GACC coupled to a ring resonator

3.1 Trapping light in the ring resonator

The asymmetric coupling of the complex GACC leads to unusual and interesting functionalities if the input and the output of the guide #2 in Fig. 1(a) are connected together. For such a condition, the upper guide becomes a ring resonator, which can be excited through the A-GACC. This ring structure is depicted in Fig. 1(b). If the grating is described by Eq. (1),

#6760 - $15.00 US Received 4 March 2005; revised 27 April 2005; accepted 27 April 2005

a signal launched into Port A will be coupled into the ring through Port C according to Eq. (9) when $S = +1$. The signal will then propagate from Port C to Port B where it will not be able to leave the ring because of the asymmetric transmission. Therefore, the signal will then be trapped in the ring.

The portion of the ring outside the grating could have a different propagation constant than the guide #2, for instance due to the DC contributions of the grating. It will be referred as the guide #3, which has its own length (L_3), propagation constant (β_3), loss coefficient (α_3), transmission in amplitude (T_3) and phase (ϕ_3). The amplitude transmission coefficient of the complete ring is given by:

$$T_r = T_2 T_3 = \exp\left[-\left(\alpha_2 L + \alpha_3 L_3\right)\right], \tag{10}$$

and will be considered as frequency independent as T_1 and T_2. Under the assumption that neither the guide #2 nor the #3 has chromatic dispersion, the phase contributions for one roundtrip in the ring can be written as a linear phase term in angular frequency:

$$\begin{aligned} \psi_r &= \psi_2 \psi_3 = \psi_{r,0} \exp\left[j(\omega - \omega_0)\tau_r\right] \\ \psi_{r,0} &= \exp\left[j\left(n_{eff,2} L + n_{eff,3} L_3\right)\omega_0 / c\right], \\ \tau_r &= \frac{n_{g,2} L + n_{g,3} L_3}{c} \end{aligned} \tag{11}$$

where τ_r is the group delay required to perform one roundtrip in the ring. Assuming an ideal A-GACC in state $S = +1$ (see Eq. (9)) and no initial signal initially trapped in the ring, (the input at Port B is zero) the output at Port D can easily be obtained:

$$\overline{E}_D = T_1 \psi_1 \overline{E}_A . \tag{12}$$

It is not as straightforward to deduce what is the field trapped in the ring. It is a combination of the field that is incident at Port A and then transferred to Port C, as well as the field that had been transferred earlier in the ring and which had time to complete one or more roundtrip up to N:

$$\overline{E}_C = 2 j \kappa L \operatorname{sinc}\left(\Delta\tilde{\beta} L\right) T_{avg} \psi_{avg} \psi_{-g} \sum_{n=0}^{N} \left(T_r \psi_r\right)^n \overline{E}_A^{(n)} , \tag{13}$$

where the "(n)" on the input field indicates how many roundtrips the signal has experienced in the ring. Therefore, before calculating its Fourier transforms $\overline{E}_A^{(n)}$, a signal longer than the roundtrip time in the ring has to be truncated. This is identical to discretizing the time in N windows of τ_r duration and subsequently propagating them.

3.2 Releasing the trapped light

As was already mentioned, the state of the A-GACC can be switched into the two other distinct states: $S = 0$ and -1. The grating with no imaginary modulation ($S = 0$) reduces the A-GACC to a standard GACC. For such a case, it is possible to transfer the signal from Port B to Port D and practically extract the signal from the ring (i.e. without leaving a signal in Port C). According to Eq. (3), a complete transfer to Port D is possible only if $\tilde{\alpha}_-$ equals zero. The only mean to achieve this, assuming both guides experience the same DC loss, is at the phase-match condition (i.e. when $\Delta\tilde{\beta} = 0$) with $\kappa L = \pi/2$ (or other solutions of $\cos(\kappa L) = 0$). However, the entire signal cannot exactly fulfill the phasematch condition. While a major portion of the signal is extracted, the rest performs a few roundtrips in the ring before coming out at Port D as weak distorted signals. It is then assumed that the ring will switch back to $S = +1$ after τ_r. Based on this assumption, the signal extracted from the ring is the following:

$$\overline{E}_D = -j \kappa L \operatorname{sinc}\left(\tilde{\gamma} L\right) T_{avg} \psi_{avg} \psi_{+g} \overline{E}_B , \tag{14}$$

For the reminder of the paper, this grating state will be labeled as the "extractor" state, while the grating state *S=+1* described by Eq. (9) will be referred as the "injector" state.

#6760 - $15.00 US Received 4 March 2005; revised 27 April 2005; accepted 27 April 2005

The complex grating with state *S*= *-1* reverses the asymmetric transmission of the A-GACC. For such case, it is possible to extract the signal from Port B to Port D without removing it from the ring. Using Eq. (9), the signal at Port C is:

$$\overline{E}_C^{(p)} = T_2 \psi_2 \overline{E}_B^{(p)}, \tag{15}$$

where "(p)" indicates the number of roundtrips completed in the ring since the A-GACC switched to the *S*= *-1* state. The signal trapped in the ring is then attenuated at each roundtrip: it acquires a phase shift, including time delay and even dispersion. An exact reconstruction of the signal at Port D has to sum over all the roundtrips performed in the ring from the moment the A-GACC has switch from *S*= *+1* to *S*= *-1*:

$$\overline{E}_D^{(P)} = -2 j\kappa L \operatorname{sinc}\left(\Delta\tilde{\beta} L\right) T_{avg} \psi_{avg} \psi_{+g} \overline{E}_B^{(0)} \sum_{p=0}^{P} (T_r \psi_r)^p , \tag{16}$$

where $\overline{E}_B^{(0)}$ is the signal at Port B just when the A-GACC switched state. The *P* indicates the duration the grating remains in state *S* = -1 in terms of the maximum number of roundtrips allowed in the ring (the actual time is $P\tau_r$). For such a state, the functionality is more like a signal duplicator than a signal extractor. For the rest of the paper, this grating state will be labeled as the "duplicator" state.

4. Temporal dynamics of the A-GACC coupled to the ring resonator

4.1 Propagation within the ring resonator

Using the complete description of the spectral characteristics of the A-GACC coupled to the ring resonator permits exploration of the temporal dynamics of such a device. The signal launched into Port A can be presented as a train of pulses in the following way:

$$E_A(t) = \sum_m \phi(t - mt_R) \exp\left[- j\omega_0 (t - mt_R)\right], \tag{17}$$

where ϕ is the pulse envelope, t_R is the time between each pulse. The fields at the output of the A-GACC can be obtained through the application of Eq. (12) and Eq. (13). This requires calculating the signal in the spectral domain using the Fourier transform of Eq. (17):

$$\overline{E}_A(\omega) = \sum_m \overline{\phi}(\omega - \omega_0) \exp\left[j\omega m t_R\right]. \tag{18}$$

It is now possible to evaluate the signal coming from Port A to Port D using Eq. (12):

$$E_D(t) = T_1 E_A(t - \tau_1). \tag{19}$$

Therefore, the signal at Port D only suffers propagating losses in the grating along the guide #1 and is retarded by the time required to propagate in that guide which has a group index of $n_{g,1}$

In the Fourier domain, the spectrum of the signal inside the ring at Port C is related to the signal at Port A by Eq. (18), which leads to:

$$\overline{E}_C = 2 j\kappa L \operatorname{sinc}\left(\Delta\tilde{\beta} L\right) T_{avg} \psi_{avg} \psi_{-g} \overline{\phi}(\omega - \omega_0) \sum_m (T_r \psi_{r,0})^{n_m} \exp\left[j\omega m t_R + j(\omega - \omega_0) n_m \tau_r\right], \tag{20}$$

where n_m is the number of roundtrips in the ring undergone by the m^{th} pulse in the input train. The signal at Port C can be obtained by taking the inverse Fourier transform of Eq. (20):

$$E_C(t) = \sum_m (T_r \psi_{r0})^{n_m} \phi_{inj}\left(t - mt_R - n_m \tau_r - \tau_{avg}\right) \exp\left[jm\omega_0 t_R\right],. \tag{21}$$

where $\tau_{avg} = (\tau_1 + \tau_2)/2$ and ϕ_{inj} is the convolution of one pulse with the grating spectrum:

$$\phi_{inj}(t) = \frac{j2\kappa L}{2\pi} T_{avg} \psi_{avg,0} \psi_{-g} \int_{-\infty}^{\infty} \operatorname{sinc}\left(\Delta\tilde{\beta} L\right) \overline{\phi}(\omega - \omega_0) \exp\left[- j\omega t\right] d\omega . \tag{22}$$

Eq. (21) shows the impact on the pulses associated with the number of roundtrips n_m they complete in the ring. They are attenuated by $T_r^{n_m}$, shifted in phase by $\psi_{r,0}^{n_m}$, and delayed by

#6760 - $15.00 US Received 4 March 2005; revised 27 April 2005; accepted 27 April 2005

$n_m\tau_r$. The effects induced by the limited bandwidth of the grating are given by Eq. (22). They are not obvious at first glance because they depend on the bandwidth of the pulse itself.

Nevertheless, it is possible to get an approximate analytical solution for a specific pulse if its spectral width is much smaller than the spectral width of the *sinc*-transfer function. Let $G(t;t_0,\delta\omega)$ be the complex amplitude of a Gaussian pulse with an energy normalized to 1 ($\int |G(t)|^2 dt = 1$), a FWHM of $2(\ln 2)^{1/2} t_0$ and a carrier angular frequency of $\omega_0 + \delta\omega$. Under the approximation of a narrowband pulse close to the phasematch condition, the *sinc* function can also be approximate by a Gaussian: $\mathrm{sinc}(x) \cong \exp(-x^2/6)$. The transfer of the input Gaussian pulse switched through the A-GACC according to Eq. (22) can now be solved analytically:

$$\phi_{inj}(t) \cong j\psi_{\pm g}\psi_{avg,0}\left\{\frac{2\kappa L}{\Gamma_{inj}} T_{avg} \exp\left[-\theta_{inj}^2/6\Gamma_{inj}^2\right]\right\} G(t;\Gamma_{inj}t_0,\delta\omega_{inj}), \tag{23}$$

The term in the curly brackets is the amplitude amplification coefficient. The pulse shape remains Gaussian, but the pulse broadens by a factor $\Gamma_{inj} = \left(1+\tau^2/3t_0^2\right)^{1/2}$ and its carrier angular frequency shifts by $\delta\omega_{inj} = -\theta\tau/3\Gamma^2 t_0^2$. Under this assumption, the pulse does not undergo dispersion and remains unchirped. Other pulse shapes with wider spectrum than the Gaussian would suffer more modifications than what is presented here. Finally, note that, for the sake of simplicity, Eq. (23) has been written in the realistic situation where the loss/gain in guides #1 and #2 are the same, $\alpha_1 = \alpha_2$, which implies a real phasematch condition $\Delta\tilde{\beta}$.

4.2 Access to the trapped signal

Once the signal is trapped within the ring resonator, one can now attempt to access it. When such an attempt is made, it is assumed that no incoming signal is launched in Port A. The available mechanisms to achieve this have already been discussed in subsection 3.2. However, it is important to point out that the switching of the imaginary grating must be timed carefully in order to access the entire pulse train.

The signal coming out at Port D is obtained by convoluting the signal trapped in the ring at Port B. Since the mathematical description only provides the signal at Port C, as shown in Eq. (20), the signal at Port B must be deduced by counter-propagating the signal at Port C obtained in the case where the A-GACC would have remained in the injection state (i.e. in the bar state). This backward propagation in the grating is done by dividing the signal at Port B by $T_2\psi_2$. As for the injected signal, the duplication and extraction is only considered here for a train of identical pulses when they have been injected at Port A.

For the case of signal duplication, Eq. (16) and (21) lead to this signal coming out of Port D:

$$E_D^{(dup)}(t) = \sum_m \sum_{p=0}^{P} (T_r\psi_{r0})^{p+n_m} \phi_{dup}(t - mt_R - (p+n_m)\tau_r - \tau_1)\exp[jm\omega_0 t_0], \tag{24}$$

which is a sum of pulses with identical shape but different amplitude and phase. The output signal is constituted of $P + 1$ pulse trains. Since the signals are only duplicated, they continue to undergo roundtrips within the ring resonator. The modifications on the pulse shape are grouped in ϕ_{dup} :

$$\phi_{dup}(t) = \frac{4\kappa^2 L^2}{2\pi} T_1\psi_{1,0} \int_{-\infty}^{\infty} \mathrm{sinc}^2\left(\Delta\tilde{\beta}L\right)\bar{\phi}(\omega-\omega_0)\exp[-j\omega t]d\omega . \tag{25}$$

In the case of signal extraction, the output in extraction state is then simply a sum over all the pulses trapped in the ring:

$$E_D^{(ext)}(t) = \sum_m (T_r\psi_{r0})^{n_m} \phi_{ext}(t - mt_R - n_m\tau_r - \tau_1)\exp[jm\omega_0 t_R]. \tag{26}$$

#6760 - $15.00 US Received 4 March 2005; revised 27 April 2005; accepted 27 April 2005

where the convolved pulse under the actions of the grating is given by:

$$\phi_{ext}(t) = \frac{2\kappa^2 L^2}{2\pi} T_1 \psi_{1,0} \int_{-\infty}^{\infty} \mathrm{sinc}\left(\Delta\tilde{\beta}L\right)\mathrm{sinc}(\tilde{\gamma}L)\bar{\phi}(\omega-\omega_0)\exp[-j\omega t]d\omega . \quad (27)$$

In general, the impact of the grating on the pulse shape has to be computed numerically either for the duplication or the extraction state. Some more physical insight could be extracted from these two integrals by assuming the same narrowband Gaussian pulse near phasematch used in Eq. (23). Under this approximation, the pulse shape obtained through the duplicator state (Eq. (25)) and the extractor state (Eq. (27)) can be written in a similar manner:

$$\phi_{out}(t;T_{out},f) \cong \psi_{1,0}\left\{\frac{4\kappa^2 L^2}{\Gamma_{ext}} T_1 T_{out}\exp\left[-(1+f)\theta^2/6\Gamma_{out}{}^2\right]\right\} G(t;\Gamma_{out}t_0,\delta\omega_{out}), \quad (28)$$

with $\Gamma_{out} = \left[1+(1+f)\tau^2/3t_0^2\right]^{1/2}$ and $\delta\omega_{out} = -(1+f)\theta\tau/3\Gamma_{out}{}^2 t_0^2$. If the duplicator state is used to access the signal trapped in the ring, both T_{out} and f equal 1. On the other hand, if the extractor state is used, and the whole pulse spectrum is close to the phasematch such as $\kappa L >> \Delta\tilde{\beta}L$, they are instead given by $T_{out} = \mathrm{sinc}(\kappa L)/2$ and $f = 3[1-\kappa L\cot(\kappa L)]/\kappa^2 L^2$. As for the study of the injection, the results presented have been simplified under the assumption of equal gain/loss in guide #1 and #2.

One interesting feature of Eq. (28) is the resulting pulse shape duration. For the duplicator state the pulse broadening is given by $\left[1+2\tau^2/3t_0^2\right]^{1/2}$ while for the extractor state the pulse broadening is given by $\left[1+(1+f)\tau^2/3t_0^2\right]^{1/2}$. For the case of the grating strength $\kappa L = \pi/2$, the factor is evaluated to $f = 12/\pi^2 \approx 1.22$. Therefore, the extracted signal is slightly longer than the duplicated one. This can be explained by the fact that an A-GACC has a broader bandwidth than a standard GACC. The duplicator state also delivers more power to the output pulse and allows repeating the same series of pulses with a period τ_r.

5. Application of an A-GACC coupled to a ring resonator

The generality and simplicity of Eq. (24)-(28) allows the exploration of the temporal dynamics of the A-GACC coupled to the ring resonator. There are three characteristic times that appear in the time arguments of Eq. (24) and Eq. (26): the time between each coupled pulses t_R, the time delay associated with the propagation in guide #1 τ_1 and the time it takes to make one full circulation in the ring τ_r. For a fixed switchable A-GACC structure, the only adjustable parameter left is t_R. Considering that the pulse duration t_0 is much shorter than these times, the dynamics will therefore be set by the relation between t_R and τ_r. Two interesting time regimes arise from such considerations: the one for which $t_R << \tau_r$ and the one for which $t_R \approx \tau_r$. The former operation regime will be referred as the "memory regime" and the latter as the "retiming regime". These two regimes are investigated in the next two subsections.

5.1 Memory cell

The basic function of the A-GACC with a ring resonator is a dynamic memory cell. After a train pulse is coupled into the ring, it will circulate inside until it is dissipated or extracted. As explained before, the only restriction is that the total duration of the signal must be less than the time for a single pulse to accomplish a roundtrip inside the ring, which means that all m pulses undergo the same number of roundtrips n_m during the injection state. As it was described in Section 2, the signal can now be accessed either by extracting it or by duplicating it and be returned in the photonic circuit. The switching must occur when the signal is performing a roundtrip in the ring before it reaches Port B or after it leaves Port C.

In order to describe graphically this application, a train of six pulses is considered, with pulse duration of t_0 = 3.6 ps and the time between each pulse of t_R = 25 ps. The summation

#6760 - $15.00 US Received 4 March 2005; revised 27 April 2005; accepted 27 April 2005

over the index *m* will be done from 0 to 5 (total of six pulses). Each pulse within the train can carry a bit of information encoded by pulse amplitude, phase or, in digital case, by missing some pulses in the train, where the pulse presence is a logical unit, and its absence is a logical zero (e.g., RZ coding schemes). The physical parameters of the A-GACC are the same as the ones used for Fig. 2, except for the DC loss, which is 0.6 dB/cm (which is state of art now for planar waveguides) in all three guides. The length of guide #3 is assumed to be 35 mm and its constant of propagation is the same as guide #2.

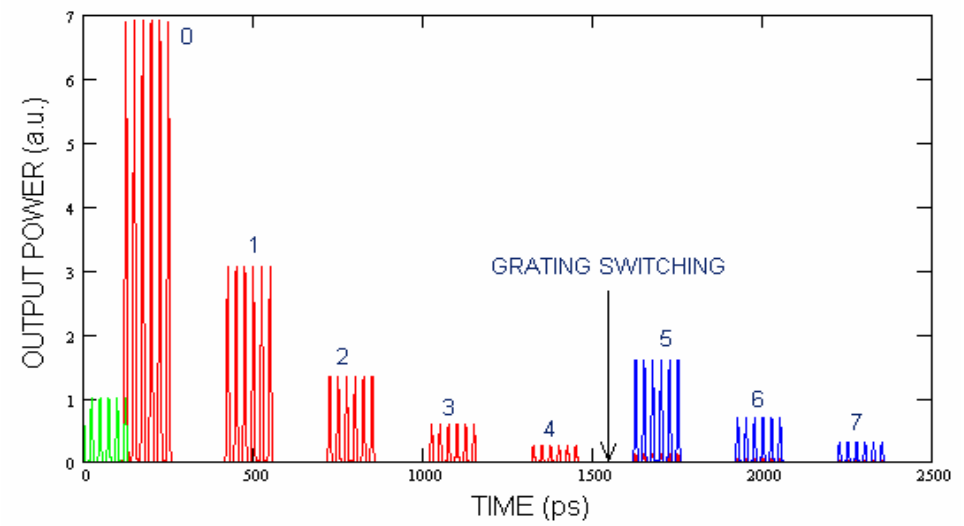

Fig. 3. Pulse train in the ring at Port C (red) and the train released from the ring after four full roundtrips inside the ring (blue) compared to the input signal (green).

The result of pulse duplication from the ring is presented in Fig. 3. The duplication was achieved by switching the imaginary part of the complex grating after four circulations of the train inside the ring, i.e. n_m=4. It is interesting to note from Eq. (24) and Fig. 3 that until the state of the grating is switched back to the injection state, the ring will provide a continuous train of pulses each separated by the roundtrip rime τ_r. This is due to the fact that the duplication of the signal does not remove the trapped signal. Therefore, it continues to circulate within the ring. When the circulating signal comes back to Port B, it is again duplicated toward Port D. In Fig. 3, the time delay between each consecutive train is τ_r = 301.016 ps. The number of circulations is marked near each train in Fig.3. Of course, the amplitude of each signal train decays with each additional roundtrip in the ring since the losses are cumulative within the ring. One interesting feature that is worth noticing is the fact that even after four roundtrips inside the ring where the signal suffers propagation losses, the duplicated signal is still more intense than the injected signal. This is the result of the double amplification that occurs during the injection/duplication operation: the first one occurs when the pulses are coupled into the ring and the second one, when they are duplicated. These results have been obtained using the approximated formula of Eq. (24) and Eq. (28). They are within 8% accuracy in respect to the accurate numerical computation using a fast Fourier transform algorithm. The main source of error is related to the Gaussian approximation of the grating spectral response.

It is interesting to consider the case where only one replica of the train is required. For such a case, the complex grating should be switched back into the injection mode just after the first release. Obviously, the main limitation for this operation is the time response of the process responsible for creating the imaginary grating. This time response is required to be at least shorter than the roundtrip time τ_r inside the ring. The choice of material should be carefully considered when designing an A-GACC that would allow such operation.

#6760 - $15.00 US Received 4 March 2005; revised 27 April 2005; accepted 27 April 2005

The signal extraction can be achieved by switching off the imaginary part of the grating. The coupler then become a standard GACC with the grating strength $\kappa L = \pi/2$. The signal extracted will not be as strong as for the duplication state since it will not undergo amplification during the extraction. It is important to mention that the extraction process is not a perfect one. If the grating strength is adjusted to $\kappa L=\pi/2$, the maximum of extraction will be reached for the wavelength associated to perfect phasematch. Even though the extraction state allows the clearing of the signal from the ring, one must understand that small remnants of the distorted pulse train will be left in the ring and will decay due to the ring losses.

5.2 Pulse retiming

The A-GACC coupled ring can also be used for pulse repetition rate multiplication or pulse retiming. The retiming regime can be demonstrated, if the time between each injected pulse train t_R is slightly lower/higher than the time of the single full circulation in the ring τ_r. Each pulse then undergoes one more/less roundtrip in the ring under the injection state than its neighbors, which means $n_{m+1} = n_m + 1$. In this case, the next coupled pulse will be added right before/after the previous injected pulse that at that time will have completed a roundtrip inside the ring. A careful adjustment of t_R can provide pulse retiming within a broad time range.

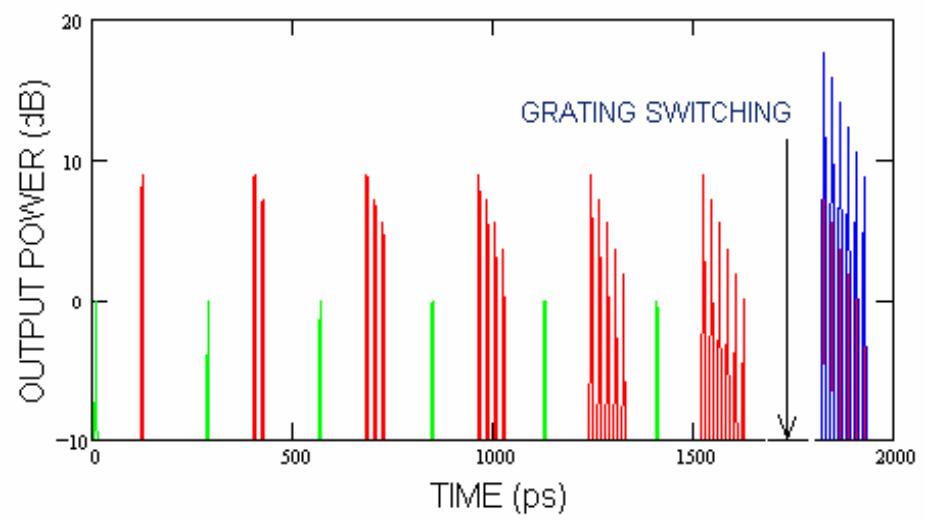

Fig. 4. Demonstration of pulse train retiming from a repetition rate of t_R = 280 ps (in Port A) to $t_R \approx 20$ ps inside the ring (red). The retimed train of six pulses duplicated into output Port D (blue) along with the input pulse (green).

An example of such functionality is demonstrated in Fig. 4 where t_R is 280 ps and t_0 is 1.8 ps where the field inside the ring is shown as a function of time. Computation has been done for losses that are half the value used for the memory cell, i.e., 0.3 dB/cm. One can see that the number of pulses accumulates in the ring from one to six as expected. Unfortunately, each pulse has decreased amplitude. This is due to the fact that each time a new pulse is added to the signal train, the previous pulses have suffered losses proportional to the number of roundtrips they have made. After accumulating six retimed pulses, the train is duplicated into output Port D by switching the grating. This produces the blue pulse train in Fig. 4. Practically all pulses in the train have amplitudes much higher than the input pulse in green. The retimed train will be amplified (more than seven times) at the moment of releasing it from the ring into Port D. Obviously, the pulse amplitudes will be more equalized if losses in the ring are reduced.

#6760 - $15.00 US Received 4 March 2005; revised 27 April 2005; accepted 27 April 2005

6. Conclusions

In this paper, we have reported a generalized study of the ring resonator unidirectionally coupled with the bus waveguide through a matched periodic modulation of both the refractive index and gain/loss of the media. We have shown how the unique spectral characteristics of the design allow light to be trapped in the ring with its amplification during this coupling process. Besides the state that traps light in the ring, a second one is responsible for releasing light from the ring, while at the same time preserving the light in the ring. Finally, the third state turns the complex grating into a conventional one of the index modulation that completely removes the light from the ring at the resonance wavelength.

We presented and rigorous framework to reconstruct correctly the signals trapped and released by this device. A first order study on the impact of the grating on narrowband Gaussian pulses provides insight on the drawbacks on the pulse shape. Finally, two applications for the A-GACC with a ring resonator have been presented: the memory cell and the pulse retiming.

Acknowledgments

This work was supported by the Natural Sciences and Engineering Research Council (NSERC) and industrial and government partners, through the Agile All-Photonic Networks (AAPN) Research Network.

#6760 - $15.00 US Received 4 March 2005; revised 27 April 2005; accepted 27 April 2005